GaussMarbles: Spherical Magnetic Tangibles for Interacting with Portable Physical Constraints

Han-Chih Kuo[*] **Rong-Hao Liang**[†] **Long-Fei Lin**[*] **Bing-Yu Chen**[†]
[*†]National Taiwan University
[*]{andikan,andln}@cmlab.csie.ntu.edu.tw [†]{rhliang,robin}@ntu.edu.tw

ABSTRACT
This work develops a system of spherical magnetic tangibles, *GaussMarbles*, that exploits the unique affordances of spherical tangibles for interacting with portable physical constraints. The proposed design of each magnetic sphere includes a magnetic polyhedron in the center. The magnetic polyhedron provides bi-polar magnetic fields, which are expanded in equal dihedral angles as robust features for tracking, allowing an analog Hall-sensor grid to resolve the near-surface 3D position accurately in real-time. Possible interactions between the magnetic spheres and portable physical constraints in various levels of embodiment were explored using several example applications.

Author Keywords
Magnetic tangibles, physical constraints, analog Hall-sensor grid, GaussSense.

ACM Classification Keywords
H.5.2. Information Interfaces and Presentation (e.g. HCI): User Interfaces

INTRODUCTION
A ball is a generic tangible object that has various uses. It is mostly used in games, where the play of the game follows the ball as it is hit or thrown by players [5]. When a skilled player applies force to a ball, it rolls, spins, bounces, or stops in a predictable way. To further control a ball, physical constraints (as in a pinball machine) are usually applied to it. The physical boundaries enrich the gaming experience by increasing kinesthetic awareness and providing haptic feedback [12], while confining the movement to prevent its falling outside the range of play [9].

To detect the precise movement of a ball within physical constraints, most related works have used external cameras to track the ball within static [10] or or dynamic constraints [4]. Portico [1] tracks a ball on a screen and the surrounding surface using two cameras that are positioned above a portable display. However, since optical detection methods are prone to interference by occlusions that are introduced by the physical constraints, the users hands, or both, the external cameras are usually mounted above the areas of interaction, making the form factors of the interaction platform less portable. Attaching an analog Hall-sensor grid [8] to the bottom of a platform improves the form factors for portability, because the sensor platform is entirely hidden from the users. Additionally, this setup is calibration-free and more robust than optical tracking, because tracking a magnetic tangible in non-ferrous physical constraints does not suffer from occlusion [7]. However, precisely tracking a spherical magnetic in a consistently high speed is challenging because the magnetic field of a rolling magnet changes with the orientation of the dipole vector. Although previous work [7] have used images of the magnetic field to infer information about either the tilt (pitch, yaw) or roll of a magnet, the non-smooth transitions between the tilt- and roll-tracking mechanisms may reduce the precision of tracking.

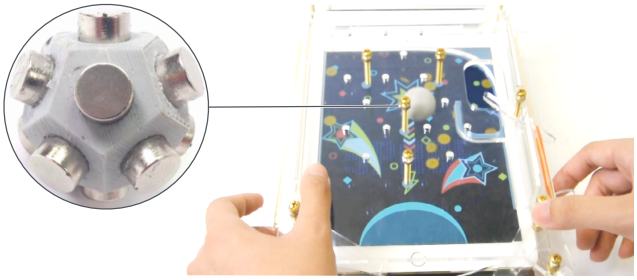

Figure 1. ***GaussMarbles* is a system of spherical magnetic tangibles for interacting with portable physical constraints.**

This work develops *GaussMarbles* (Figure 1), which is a system of spherical magnetic tangibles for token+constraint interactions [12] on portable platforms. To overcome the computational challenges of tracking spherical magnetic tangibles in 3D, their magnetic fields are shaped using a regular polyhedron. This design makes the magnetic fields of the tangibles more spherically symmetric as the objects roll/bounce on a surface, respond to physical constraints or are lifted by hands, enabling an analog Hall-sensor grid to track the near-surface 3D position precisely in real time. Several applications have demonstrated a rich set of interactions between GaussMarbles and physical constraints in various levels of embodiment [3], including interactions on, above, nearby, and distant from computer displays.

DESIGNING SPHERICAL MAGNETIC TANGIBLES

Challenges of Sensing Spherical Magnetics
Accurately tracking the 3D position of a rollable spherical tangible in a consistently high speed is challenging because the orientation of its dipole vector changes as it rolls and bounces. Figure 2 shows that the distribution of the magnetic

CHI'16, May 07-12, 2016, San Jose, CA, USA
 ISBN 978-1-4503-3362-7/16/05$15.00
DOI: http://dx.doi.org/10.1145/2858036.2858559

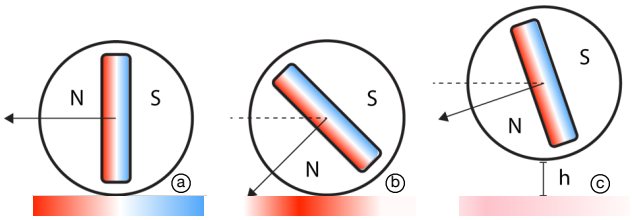

Figure 2. (a) Single-magnet ball. (b) When the ball rolls on the plane, the S-pole component of the magnetic field becomes invisible at a tilt angle $\theta_{h=0}$. (c) When the ball hovers above the plane, the S-pole component becomes invisible at a tilt angle $\theta_{h>0}$.

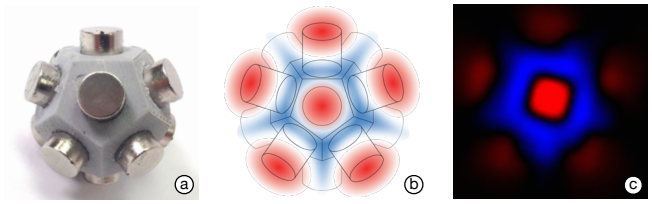

Figure 3. (a) Shaping a magnetic field using a magnetic polyhedron. (b) Schematic and (c) measured bipolar magnetic fields.

field of a rolling magnetic ball (or a ball that contains a flat disc magnet) changes with the orientation of its dipole. When a magnetic ball is placed on a sensing plane ($h = 0$) such that the N(orth)-or S(outh)-pole vector is parallel to it, both the N- and S-parts of its magnetic field are visible, so the 3D position of the ball can be resolved from the relative positions and intensities of the N-and S-pole components, using the sensing algorithm that is proposed in GaussBits [7]. However, when the dipole vector is tilted at a specific angle $\theta_{h=0} > 0$ toward the N-pole, the S-polar magnetic field becomes invisible to the sensor, so the same algorithm no longer works. When the magnetic ball is lifted above the surface in a height $h > 0$, and the S-polar magnetic field becomes invisible to the sensor at a specific angle $\theta_{h>0}$ toward the N-pole. from the N-pole. Since magnetic field is not spherically symmetric, $\theta_{h>0}$ is not equal with $\theta_{h=0}$, and θ varies with h. Without a reliable and efficient way to determine the tilt angle θ, of the dipole vector in all directions, the position of ball along the z-axis cannot be determined.

Shaping the Magnetic Fields Using A Regular Polyhedron

In other studies, analytic solutions and specific sensors (e.g., [11]) are used to approximate the 3D position of a magnetic tangible; in this study a simpler but more generic method is used to simplify the computational challenge: the magnetic field is caused to be almost spherically symmetric by deploying equal-strength magnets on a regular polyhedron to eliminate the need to resolve the tilt angle θ. Regular polyhedrons are chosen because they have the following three important properties. (1) The vertices of a polyhedron all lie on a sphere. (2) All of the dihedral angles of a polyhedron are equal. (3) All of the vertex figures of a polyhedron are regular polygons. As in GaussBricks [6], magnets with the same poles of equal strength were mounted on the center of each face of a regular polyhedron, and the resulting bi-polar magnetic fields were expanded in equal dihedral angles, making the components of both the N- and S-polar fields visible to the sensors at all times, as shown in Figure 3.

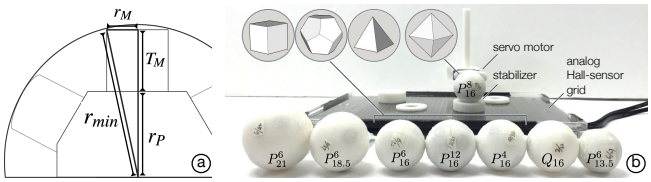

Figure 4. (a) Model of a magnetic-polyhedron sphere. (b) Experimental Apparatus.

Regular polyhedrons with 4, 6, 8, 12, and 20 faces can be used to build magnetic spheres. To ensure that a spherical magnetic tangible rolls in a natural and predictable way, the magnetic polyhedron must be placed at its center. Figure 4a shows the model of such magnetic spheres. Consider a target regular polyhedron. Consider a target regular polyhedron P, with an inner-scribe sphere radius of r_P. A cylindrical magnet M is mounted on the center of each face of the polyhedron, where r_M is the radius of the magnet and T_M is its thickness. The minimal radius r_{min} of the sphere then can be obtained as $r_{min} = \sqrt{(r_P + T_M)^2 + r_M^2}$. In practice, a sphere case C is required to protect the polyhedron on which the magnets are mounted. If T_C is the thickness of the case, then the radius of a sphere r with a case of radius r_{min} is obtained as $r = r_{min} + T_C$, where $T_C \geq 0$.

EXPLORATIVE STUDY

A series of formal measurements were made to establish parameters for an effective design. Since using magnets of larger thickness T_M and/or radius r_M results in stronger magnetic fields and more stable tracking, the effects of two other parameters are studied herein — (1) the *number of faces*, and (2) the *size of the faces of the magnetic polyhedron* — to obtain a suitable tracking algorithm.

Apparatus: As shown in Figure 4b, eight magnetic spheres were fabricated using a 3D printer. Seven of them, P^6_r and P^n_{16}, where $r = \{13.5, 16, 18.5, 21\}$ and $n = \{4, 6, 8, 12\}$, are r mm-radius spheres that contains of a n-face magnetic polyhedron in each sphere; the other one, Q_{16}, is a 16mm-radius sphere that contains a single 12.5mm (radius) × 3mm (height) cylindrical magnet. At the centers of the faces of each magnetic polyhedron are mounted neodymium magnets of 4mm (r_M) × 8mm (T_M) such that the N(orth)-poles face outward. The case thickness (T_C) of each sphere was 0.5mm.

To capture images of the magnetic field, a 32×32 = 1024 Winson WSH138 analog Hall-sensor grid with a 16(W)×16(H) cm^2 sensing area is used. Each sensor element detects the intensities of both N-and S-polar magnetic field components from 0 to 200 Gauss on a 256-point scale and at a sampling rate that consistently exceeds 40 fps. The N- and S-polar magnetic field components at each sample point are mapped as various intense red or blue colors on a 310px×310px bitmap. The Hall-sensor grid is calibrated using a method that was presented previously [6]. An elevating platform, which consists of a servo motor that can rotate each ball, mounted on a base, is used to collect data.

Tasks: Each sphere is placed at five arbitrary positions on the sensor. At each position, measurements were made at four

hover heights - 3, 6, 9, and 12 mm. At each height, 10 angles between 0 and 90 degrees were set, and each measurement consists of 100 samples. The analysis included 8 (units) × 5 (positions) × 4 (hover heights) × 10 (angles) × 100 (samples) = 160,000 bitmaps of magnetic fields.

Data Processing

Each bi-polar magnetic-field image I_B comprises sub-images - I_N, which comprises only N-polar fields, and I_S, which comprises only S-polar fields. For each set of three images of magnetic fields (i.e., I_B, I_N, I_S) the distribution of the magnetic fields was observed by applying a threshold of 10 Gauss to each image for blob extraction. In searching for more effective ways to track spherical magnetics, the following three centroids are identified; (1) the *centroid of contours* (O_c): as in GaussBits [7], which is calculated as the centroid of the pixels of blobs contour. If the target image has multiple contours and contour centroids, then O_c is computed as their centroid position; (2) *centroid of pixels* (O_p): the centroid position of all pixels within all blobs is computed as $O_p = \sum_{i=0}^{N} p_i/N$, where p_i is the position of each pixel i, and N is the total number of pixels within the blobs; (3) *centroid of mass* (O_m): the centroid of the intensity-weighted pixel positions within all blobs is computed as $O_m = \sum_{i=0}^{N} v_i p_i / \sum v_i$, where p_i is the position; v_i is the intensity of pixel i, and N is the total number of pixels within the blobs.

For all collected centroids, the mean value $\bar{O}$ of all samples is firstly calculated. Then, the Euclidian distance d_i between the centroid of each sample i and $\bar{O}$ is obtained. Finally, the mean distance $\bar{d}$ and its standardard deviation of all samples is obtained as the metrics of *dispersion*. Along with $\bar{O}$ and $\bar{d}$, the blob area size A and the maximum pixel intensities M inside the blob of each image of a magnetic field are recorded.

Results and Discussions

The results thus obtained yield four major findings and guidelines for sensing spherical magnetic tangbles.

1. *The bi-polar centroid of mass ($I_B - O_M$) is the most stable feature for tracking magnetic spheres in the xy-plane.* Figure 5 shows the mean distance $\bar{d}$ of all samples obtained from the 3 (centroids: O_c, O_p, O_m)×3 (images of magnetic field: I_B, I_N, I_S) = 9 results for the 16mm-radius magnetic spheres at height $h = 3mm$. The centroid of mass in a bi-polar image (O_m-I_B) exhibits the least dispersion as the magnetic sphere rolls on the display, significantly outperforming the other features (i.e., O_c-I_N and O_c-I_B) that were used in GaussBits [7].

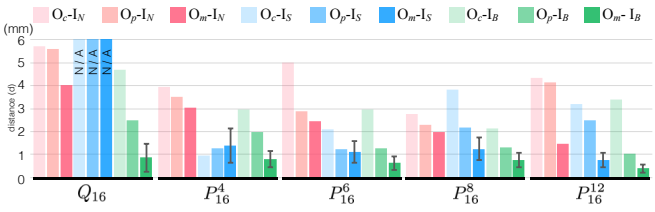

Figure 5. Using centroid of mass of a bi-polar image (O_m-I_B) is the most stable feature of positioning in the xy-plane.

2. *The magnetic polyhedrons support reliable z-axis tracking using the S-polar intensity (M_S) or the product of S-polar area and intensity ($A_S \times M_S$), whereas a single magnet does not support z-axis tracking.* Figure 6 shows the resulting M_S and $A_S \times M_S$ of the four 16mm-radius magnetic-polyhedron spheres at the heights of $h = 3,6,9,12mm$. The plotted 95% confidence interval (CI) region is that in which M_S reliably discriminates between $h = 3$ and $h = 9$ and $A_S \times M_S$ further descrimiates among$h = 3$, $h = 6$ and $h = 9$. The uses of M_S and $A_S \times M_S$ fail for the 16mm-radius single-magnet sphere because the S-polar component disappears at angle θ_h.

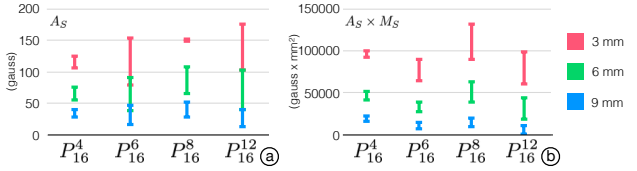

Figure 6. The hover height of the magnetic polyhedrons can be resolved by using (a) the S-polar area size (A_S) or (b) the product of S-polar area size and intensity ($A_S \times M_S$).

3. *Magnetic polyhedrons with more faces yield greater accuracy, but performance drops as sensing distance increases.* Figure 7a shows the mean distance $\bar{d}$ of (O_m-I_B) for the four 16mm-radius magnetic-polyhedron spheres at the heights of $h = 3,6,9,12mm$. Generally, the O_m of P^8_{16} are of the least degree of dispersion, because the overall magnetic field of a polyhedron with more faces is more symmetric. The 12-face magnetic polyhedron P^{12}_{16} appears to be more stable than P^8_{16} at $h = 3mm$, but the precision falls as h increases above 6mm because the N-polar blobs becomes unstable.

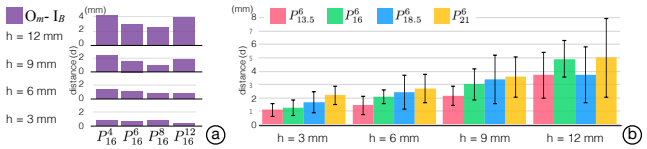

Figure 7. (a) Magnetic polyhedrons with more faces yield greater accuracy, but performance drops as sensing distance increases. (b) Smaller magnetic polyhedrons yield slightly greater accuracy.

4. *Smaller magnetic polyhedrons yield slightly greater accuracy.* Figure 7b shows the mean distance $\bar{d}$ of (O_m-I_B) for the four 6-face magnetic-polyhedron spheres at heights of $h = 3,6,9,12mm$. Larger faces result in lower accuracy, although not statistically significantly so (Z-test, all $p > 0.05$).

INTERACTING WITH PHYSICAL CONSTRAINTS

Five applications are implemented to demonstrate interactions between spherical magnetic tangibles and physical. With reference to Fishkin's taxonomy of levels of embodiment in TUI [3], interactions with physical constraints are categorized as being *on*, *nearby*, or *distant* from a display.

Interacting with Constraints on a Display

The *Pinball* game (Figure 8) illustrates the use of a physical constraint on a tablet display, iPad Air 2[1], on the back of which is attached an analog Hall-sensor grid. A physical pinball case is fixed on the display. A user launches the ball by pulling and releasing the launcher; uses the handles to hit the ball toward the target to receive a bonus score, and shakes the display to prevent the ball falling off.

[1] http://www.apple.com/ipad-air-2/

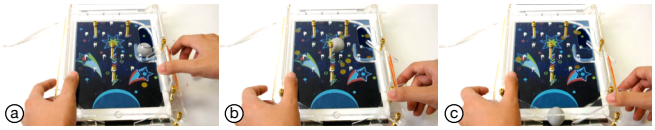

Figure 8. *Pinball* game. A user (a) launches the ball, (b) hits the ball to score, and (c) shakes the display to prevent the ball from falling off.

The *Labyrinth* game (Figure 9), which illustrates the use of a GaussMarble that is coated conductive rubber for sensing touch [2]. A maze-like cover is applied to the same display. A user releases the ball to begin playing, holds and tilts the display to move the ball around the obstacles to receive a bonus. The user can also take a shortcut by popping the ball up, but risks dropping the ball in so doing. Cheating by touching the ball is detected.

Figure 9. *Labyrinth* game. A user (a) holds the display to move the ball (b) toward the bonus to score. (c) Touching the ball is not allowed.

The *Golf putter* game (Figure 10) demonstrates using continuous territory as constraint. A transparent sheet mounted clay-made territory is applied to a 15-inch laptop display, on the back of which is attached an analog Hall-sensor grid. A user uses a golf putter to push the ball from the starting position toward the hole. Since the game reflects real-world physics, the user must putt harder to drive the ball up a hill so that it does not roll into a pond. The user can freely modify the path by including other physical objects in the game.

Figure 10. *Golf putter* game. A user (a) applies a transparent sheet mounted clay-made territory to the display. (b) The ball falls into the pond or (c) into the hole.

Interacting with Constraints nearby a Display

The *Bowling* game (Figure 11) demonstrates the use of a near-display constraint that bridges the physical object and digital content. A physical bowling lane, on the back of which is attached an analog Hall-sensor grid, is placed in front of a display that exhibit a virtual bowling lane. Between the display and the lane is a valley. After a user bowl the ball by rolling the physical ball toward the screen, the physical ball drops into the valley, and a virtual ball appears on the display, rolls along the original path until it hits the virtual bowing pins. The platform then returns the physical ball to the user along the slope underneath, so the user can freely bowl the ball again. The ball in the users hand provides rich haptic feedback, and the virtual pins on the screen do not require manual rearrangement by the user. Users enjoy both physical and digital gaming experiences.

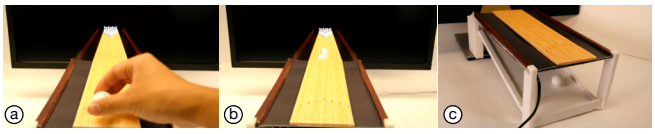

Figure 11. *Bowling* game. A user (a) rolls a physical bowling ball to (b) hit virtual pins. (c) The ball is returned to the user after the shot.

Interacting with Constraints Distant from a Display

The *Dart* game (Figure 12) demonstrates the use of a remote constraint that interacts with mobile displays. Both a dartboard and GaussMarbles are wrapped in Velcro, which functions as a material constraint that provides high friction to compensate for the low rolling friction of spheres. Multiple GaussMarbles can stick to the dartboard, and are sensed by an analog Hall-sensor grid that is attached to the back of it. A user must pair a smartphone with the dartboard, and throw balls, like darts, toward the dartboard to score. When a ball sticks to the dartboard, the smartphone shows both the results and the score, based on the position of dart. The user can either throw more balls to increase the score, or reset the game by removing the darts from the dartboard.

Figure 12. *Dart* game. A user (a) pairs a smartphone with a dart-board, (b) throws a dart to score, (c) and throws more darts.

CONCLUSION

This work developed *GaussMarbles*, which is a system of spherical magnetic tangibles for interacting with portable physical constraints. Unlike previous token+constraint systems, most of which are developed for in-hand direct manipulation and 1D interaction under strict constraints on movements [12], this work exploits the affordance of spheres for *hands-off manipulation* (such as by letting a ball roll freely) with a range of *loose constraints* from 2D to 3D, discrete to continuous, on-screen and around-screen, using low-friction to high-friction materials (such as Velcro darts). Through a series of experiments, the guidelines for designing the magnetic polyhedrons have been identified. Therefore, developers can easily replicate the results, and freely scale the system by applying the same methods on various sizes of analog Hall-sensor grids. This work provides a new perspective from which TUI researchers and practitioners can design TUIs in richer movement and various levels of embodiment, which can be exploited in the future to bring interactivity to physical ball games and make virtual ball games more physical.

ACKNOWLEDGMENTS

This work was partly supported by GaussToys Inc., Ministry of Science and Technology, National Taiwan University, and Intel Corporation under Grants NTUICRP-104R7501, MOST103-2911-I-002-001, MOST103-2221-E-002-158-MY3, MOST103-2218-E-002-024-MY3, and MOST104-2218-E-002-034.

REFERENCES

1. Daniel Avrahami, Jacob O. Wobbrock, and Shahram Izadi. 2011. Portico: Tangible Interaction on and Around a Tablet. In *Proceedings of the 24th Annual ACM Symposium on User Interface Software and Technology (UIST '11)*. ACM, New York, NY, USA, 347–356. DOI:**http://dx.doi.org/10.1145/2047196.2047241**
2. Liwei Chan, Stefanie Müller, Anne Roudaut, and Patrick Baudisch. 2012. CapStones and ZebraWidgets: Sensing Stacks of Building Blocks, Dials and Sliders on Capacitive Touch Screens. In *Proceedings of the SIGCHI Conference on Human Factors in Computing Systems (CHI '12)*. ACM, New York, NY, USA, 2189–2192. DOI: **http://dx.doi.org/10.1145/2207676.2208371**
3. Kenneth P. Fishkin. 2004. A Taxonomy for and Analysis of Tangible Interfaces. *Personal Ubiquitous Comput.* 8, 5 (Sept. 2004), 347–358. DOI: **http://dx.doi.org/10.1007/s00779-004-0297-4**
4. Sean Follmer, Daniel Leithinger, Alex Olwal, Akimitsu Hogge, and Hiroshi Ishii. 2013. inFORM: Dynamic Physical Affordances and Constraints Through Shape and Object Actuation. In *Proceedings of the 26th Annual ACM Symposium on User Interface Software and Technology (UIST '13)*. ACM, New York, NY, USA, 417–426. DOI: **http://dx.doi.org/10.1145/2501988.2502032**
5. Osamu Izuta, Toshiki Sato, Sachiko Kodama, and Hideki Koike. 2010. Bouncing Star Project: Design and Development of Augmented Sports Application Using a Ball Including Electronic and Wireless Modules. In *Proceedings of the 1st Augmented Human International Conference (AH '10)*. ACM, New York, NY, USA, Article 22, 7 pages. DOI: **http://dx.doi.org/10.1145/1785455.1785477**
6. Rong-Hao Liang, Liwei Chan, Hung-Yu Tseng, Han-Chih Kuo, Da-Yuan Huang, De-Nian Yang, and Bing-Yu Chen. 2014. GaussBricks: Magnetic Building Blocks for Constructive Tangible Interactions on Portable Displays. In *Proceedings of the SIGCHI Conference on Human Factors in Computing Systems (CHI '14)*. ACM, New York, NY, USA, 3153–3162. DOI:**http://dx.doi.org/10.1145/2556288.2557105**
7. Rong-Hao Liang, Kai-Yin Cheng, Liwei Chan, Chuan-Xhyuan Peng, Mike Y. Chen, Rung-Huei Liang, De-Nian Yang, and Bing-Yu Chen. 2013. GaussBits: Magnetic Tangible Bits for Portable and Occlusion-free Near-surface Interactions. In *Proceedings of the SIGCHI Conference on Human Factors in Computing Systems (CHI '13)*. ACM, New York, NY, USA, 1391–1400. DOI:**http://dx.doi.org/10.1145/2470654.2466185**
8. Rong-Hao Liang, Kai-Yin Cheng, Chao-Huai Su, Chien-Ting Weng, Bing-Yu Chen, and De-Nian Yang. 2012. GaussSense: Attachable Stylus Sensing Using Magnetic Sensor Grid. In *Proceedings of the 25th Annual ACM Symposium on User Interface Software and Technology (UIST '12)*. ACM, New York, NY, USA, 319–326. DOI: **http://dx.doi.org/10.1145/2380116.2380157**
9. James Patten and Hiroshi Ishii. 2007. Mechanical Constraints As Computational Constraints in Tabletop Tangible Interfaces. In *Proceedings of the SIGCHI Conference on Human Factors in Computing Systems (CHI '07)*. ACM, New York, NY, USA, 809–818. DOI: **http://dx.doi.org/10.1145/1240624.1240746**
10. Dominik Schmidt, Raf Ramakers, Esben W. Pedersen, Johannes Jasper, Sven Köhler, Aileen Pohl, Hannes Rantzsch, Andreas Rau, Patrick Schmidt, Christoph Sterz, Yanina Yurchenko, and Patrick Baudisch. 2014. Kickables: Tangibles for Feet. In *Proceedings of the SIGCHI Conference on Human Factors in Computing Systems (CHI '14)*. ACM, New York, NY, USA, 3143–3152. DOI: **http://dx.doi.org/10.1145/2556288.2557016**
11. J.T. Sherman, J.K. Lubkert, R.S. Popovic, and M.R. DiSilvestro. 2007. Characterization of a Novel Magnetic Tracking System. *IEEE Transactions on Magnetics* 43, 6 (June 2007), 2725–2727. DOI: **http://dx.doi.org/10.1109/TMAG.2007.893314**
12. Brygg Ullmer, Hiroshi Ishii, and Robert J. K. Jacob. 2005. Token+Constraint Systems for Tangible Interaction with Digital Information. *ACM Trans. Comput.-Hum. Interact.* 12, 1 (March 2005), 81–118. DOI:**http://dx.doi.org/10.1145/1057237.1057242**